JOURNAL OF SOLID STATE CHEMISTRY **137,** 87–93 (1998)
ARTICLE NO. SC977720

The Cubic/Tetragonal Phase Transition in D3C–THF: an Optical and X-ray Powder Diffraction Study

K. Knorr[1] and W. Depmeier

Mineralogisch Petrographisches Institut, Christian Albrechts Universität zu Kiel, Olshausenstr. 40, D-24098 Kiel, Germany

Received June 20, 1997; in revised form November 6, 1997; accepted November 20, 1997

The high-temperature phase transition in the clathrasil Dodecasil–3C ($17SiO_2 \cdot (CH_2)_4O$) has been studied by high-temperature, high-resolution powder diffraction and by following the temperature evolution of the optical birefringence. The transition changes the crystal system from cubic to tetragonal at 359(1) K. A detailed discussion of the symmetry properties of the phase transition is given. The transition behavior was characterized by group theoretical considerations as well as in the framework of Landau theory. The phase transition could be classified as improper ferroelastic and of first order. In addition to the tetragonal ferroelastic lattice strain, a symmetry-allowed volume reduction could be observed.

INTRODUCTION

Dodecasil–3C (D3C, in short) belongs to the group of crystalline microporous host structures, which consist of SiO_4 tetrahedra as main building units and are therefore called clathrasils (1). In D3C all-corner-connected SiO_4 tetrahedra from pentagon–dodecahedra cages (face symbol $[5^{12}]$), which are face-connected in such a way that they build pseudohexagonal nets. A cubic close packing of these nets results in a second kind of cage, the hexadecahedra (face symbol $[5^{12}6^4]$). The cages are 5.7 or 7.5 Å, respectively, in free diameter.

Structure-directing template molecules such as pyridine or trimethylamine are located in the $[5^{12}6^4]$ cages, whereas smaller molecules like CH_4 and atoms like Kr, Xe, and Ar are usually located in the $[5^{12}]$ cages. For the title compound, the template is tetrahydrofurane, $(CH_2)_4O$ (THF for short), which is located in the hexadecahedra cages.

The highest possible symmetry for the D3C topology is the space group $Fd\bar{3}m$ with the unit cell parameter $a_0 \approx 19.4$ Å (3). While small and spherical templates like CH_4, trimethylamine, or noble gases tend to stabilize D3C with cubic symmetry at room temperature (2), larger molecules force the crystallization of D3C structures, which are tetragonal (t–butylamine) or orthorhombic (pyrrolidine) at ambient conditions (8).

D3C with trimethylamine as template has been described in $Fd\bar{3}$ (4). The space group $Fd\bar{3}m$ has been given for detemplated D3C (5). For the guest molecule pyridine, the D3C structure was described in the tetragonal space group $I\bar{4}2d$ (6), whereas for pyrrolidine Fddd (8) and for tert-butylamine $I4_1/a$ (8) have been determined. D3C with the guest molecule THF (D3C-THF) has space group $I4_1/a$ at room temperature, with unit cell parameters $a = 13.684(2)$ and $c = 19.482(3)$ Å (9).

D3C shows a series of temperature-induced phase transitions. Könnecke and Fuess (8) gave the following summary of the already observed phases:

low-temperature 2
↕ ≈ 223 K
low-temperature 1
↕ 271–253 K
room-temperature phase
↕ 453–353 K
cubic high-temperature

The reported transition temperatures vary in dependence on the size of the molecule and possibly show hysteresis effects. Reversible phase transitions were reported for D3C-THF at temperatures 370 and 260 K and near room temperature from differential scanning calorimetry (DSC) and ^{29}Si magic angle spinning nuclear magnetic resonance (^{29}Si–MAS–NMR) (10). The high-temperature transition could be assigned to a tetragonal/cubic transition, which was confirmed by high-temperature powder diffraction. The cell parameters of the tetragonal I-centered cell are related to the cell parameters of the F-centered cubic cell by $a_t \approx \sqrt{2}/2 \cdot a_c$ and $c_t \approx c_c$ with the indices c and t refering to the cubic and tetragonal cell, respectively. A low-temperature synchrotron powder diffraction and NMR study (11) showed the existence of monoclinic (proposed space group

[1] Correspondence address: Dr. Karsten Knorr, Hahn-Meitner-Institut Berlin, Dept. NE, Glienicker Str. 100, D-14109 Berlin, Germany

0022-4596/98 $25.00

$C2/m$) and orthorhombic (proposed space group *Imma*) phases for D3C-THF.

The purpose of the present paper is to provide a more quantitative description of the cubic/tetragonal phase transition.

EXPERIMENTAL

Crystals were grown hydrothermally in quartz glass tubes (2). For optical experiments, an octahedrally shaped, colorless crystal of ≈ 500 μm diameter was selected and oriented along one of the pseudocubic $\langle 100 \rangle$ axes by X-ray oscillation photographs. The crystal was embedded, ground and polished to optical quality, together with a quartz crystal for the determination of sample thickness d (12). We measured the temperature dependence of the optical birefringence, applying a LEITZ heating stage. It was adapted to a ZEISS microscope-spectrometer UMSP80. The temperature was measured by a built-in Pt/PtRh thermocouple approximately 5 mm apart from the sample. The temperature was regulated using an EUROTHERM temperature controller. We noticed an offset between thermocouple and sample temperatures of about $10(\pm 5)$ K. The data were corrected correspondingly. For the determination of the path difference Γ, an Ehringhaus type 2λ compensator was used for polychromatic 'white' light. The compensation of the path difference was performed 10 times for each direction and averaged, in order to improve statistics. The optical birefringence n was determined from $n = \Gamma/d$ with a resulting error $\Delta n = (\Delta\Gamma + (\Gamma/d)\Delta d)/d$.

High-resolution powder diffraction data were collected employing a Guinier type powder diffractometer (HUBER G645) with Cu$K\alpha_1$ radiation ($\lambda = 1.54051$ Å). The resolution of the instrument was $0.04^\circ\theta$, determined at the Si(111) reflection. Diffraction patterns were collected with a step width of 0.005° and a counting time of 10 s per step. The instrument was equipped with a closed-cycle He refrigerator (CTI Cryogenics) and controlled by a Hewlett Packard microcomputer and a Lakeshore temperature controller. It allowed measurements in the range from 12 to 375 K. The temperature stability was about 0.1 K and the absolute temperature was correct within 2 K (13). The measurements were performed in the range 330–375 K in steps of 1 K. Crystals of D3C-THF were ground in an agate mortar and mixed with a small amount of Si as an internal standard. The powder was prepared between Mylar foil and fixed on a standard sample holder.

The Bragg peak positions and profile parameters were determined using the program PRO-FIT (14). The highly asymmetric peak profiles were modelled by a split-type pseudoVoigt function. The symmetric pseudoVoigt function $P(x)$ allows the refinement of a mixing parameter η, determining the fraction of Lorentzian $L(x)$ and Gaussian $G(x)$ components needed to fit the profile $P(x) = \eta L(x) + (1 - \eta)G(x)$. The split-type function consists of two functions, which are defined at the low-angle side of the peak maximum position $P(x)_L$ and the high-angle side $P(x)_H$, respectively. Highly asymmetric peaks can be modelled by the use of two different peak half widths, H_L and H_H, and the mixing parameters η_L and η_H, respectively. The resulting full width at half maximum (FWHM) is given by $H_L + H_H$. For the present data analysis we applied the constraint $\eta_L = \eta_H = \eta$.

RESULTS AND DISCUSSION

Optics

The thickness of the crystal plate is 390(1) μm. We determined the temperature dependence of the optical birefringence. Above 360 K, the sample is optically isotropic and therefore of cubic symmetry. From Fig. 1, it follows that the birefringence decreases almost continuously to zero with increasing temperature. For continuous transitions the temperature evolution of the excess property can often be described by a simple power law

$$(T_c - T)^\beta. \qquad [1]$$

This equation was fitted to the data, resulting in the exponent $\beta = 0.43(1)$ and the transition temperature $T_c = 359(1)$ K.

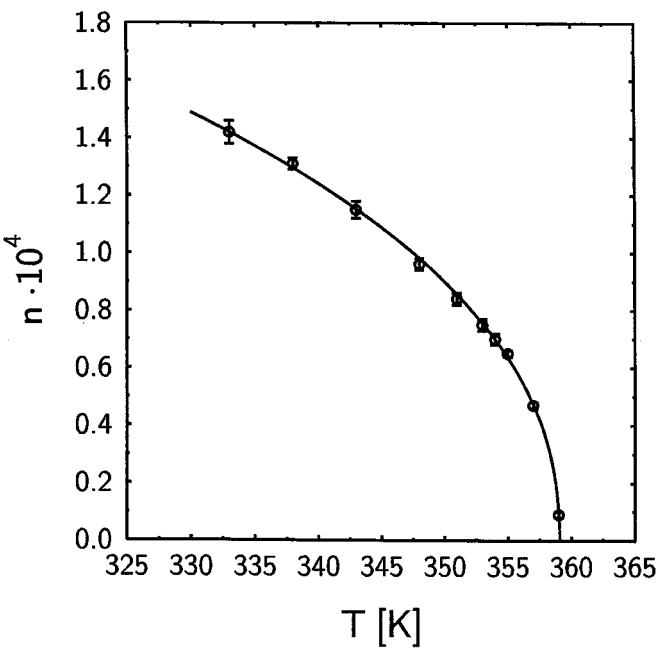

FIG. 1. Birefringence at the cubic/tetragonal transition in D3C-THF as function of temperature. The curve corresponds to the fit of Eq. [1].

X-ray Diffraction

We followed the position of the cubic 004 reflection, which is split in the room temperature phase into the tetragonal 004 and 220 reflections (Fig. 2). The intensity ratio between the two reflections is 1 : 2. This corresponds to the multiplicity of the pseudocubic (004) and (400/040) lattice planes. The temperature dependence of the cell parameters was determined for the cubic 19 Å metric of the 'para'-phase. Conventional error determination, based on the differentiation of Bragg's law, results in large errors of the cell parameters according to the low Bragg angle ($2\theta \approx 18.3^\circ$) of the reflections. Based on the uncertainty in θ of the peak fit (5×10^{-4}), we approximated the relative errors in the cell parameters and the resulting spontaneous strain to be less than 7×10^{-3} and 2×10^{-4}, respectively.

The cell parameters and volume of the unit cell are plotted in Figs. 3 and 4. The solid straight lines correspond to the extrapolated cell parameter a_0, and the volume $V_0 = a_0^3$ of the cubic phase into the tetragonal phase. The dotted curve in Fig. 3 shows the values of

$$a_0^{\mathrm{id}} = (2a_t + c_t)/3, \qquad [2]$$

which would correspond to the extrapolated cell parameter a_0 of the high-temperature phase for the case of a proper ferroelastic phase transition. A deviation of a_0^{id} from a_0 is obvious in Fig. 3. This deviation causes a reduction of the unit cell volume, which is illustrated by the deviation of the volume from V_0 (Fig. 4). Due to this volume reduction, the phase transition has to be characterized as improper ferroelastic. According to Salje (15) the symmetry-adapted scalar spontaneous strain ε is given by

$$\varepsilon = \sqrt{\left(\frac{c - a_0}{a_0}\right)^2 + 2\left(\frac{a - a_0}{a_0}\right)^2}. \qquad [3]$$

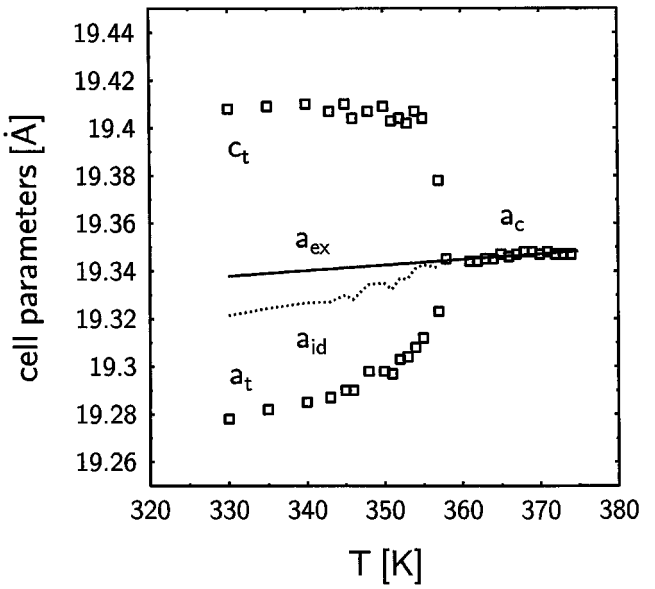

FIG. 3. Temperature evolution of the cell parameters at the cubic/tetragonal transition in D3C-THF. The straight line corresponds to the extrapolated cubic cell parameter into the tetragonal phase; the dotted line is the idea value according to Eq. [2].

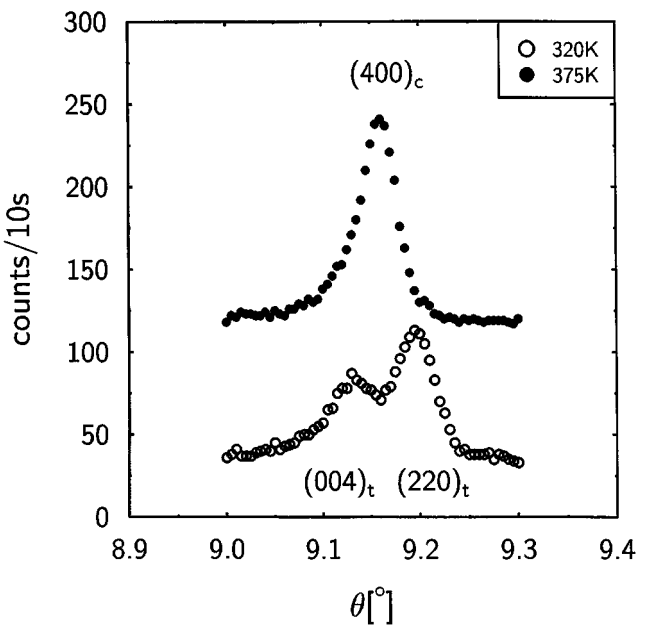

FIG. 2. Peak splitting of the cubic (400) reflection (●) into the tetragonal (004) and (220) reflections (○).

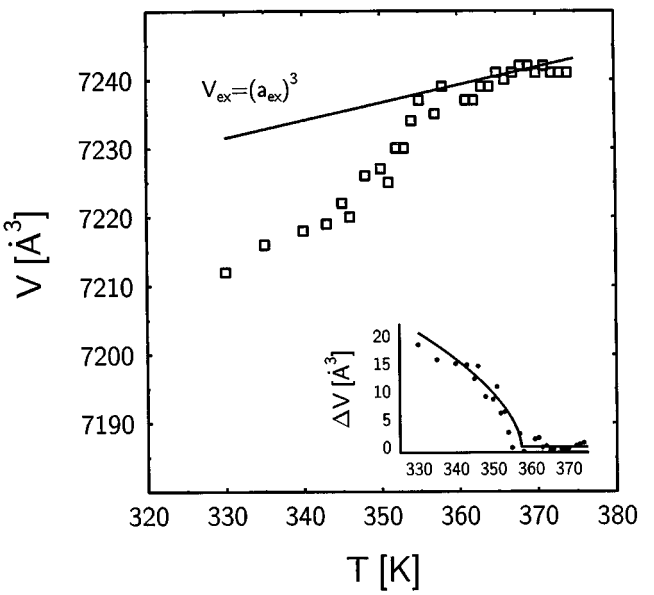

FIG. 4. Temperature evolution of the unit cell volume at the cubic/tetragonal transition in D3C-THF. The inset shows the temperature evolution of the excess volume ΔV.

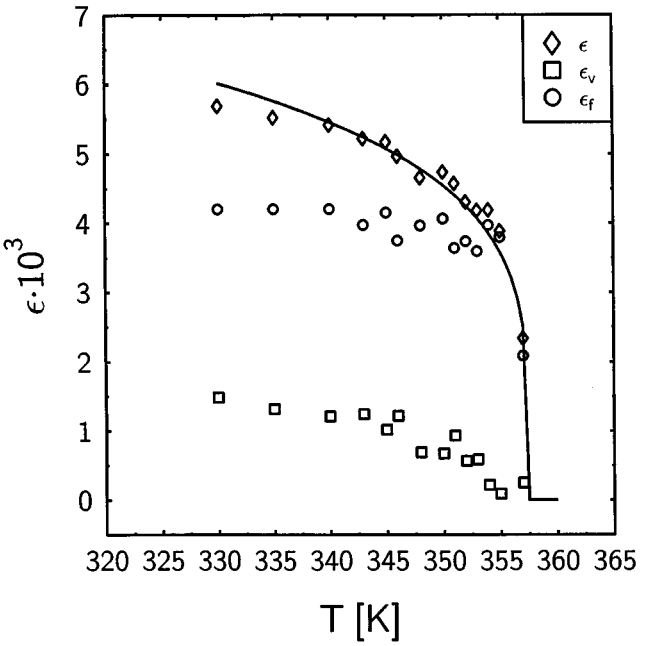

FIG. 5. Plot of total strain ε, volume strain ε_v, and pure ferroelastic strain ε_f vs temperature for the cubic/tetragonal phase transition in D3C-THF. The solid line corresponds to Eq. [1] with $\beta = 0.215$.

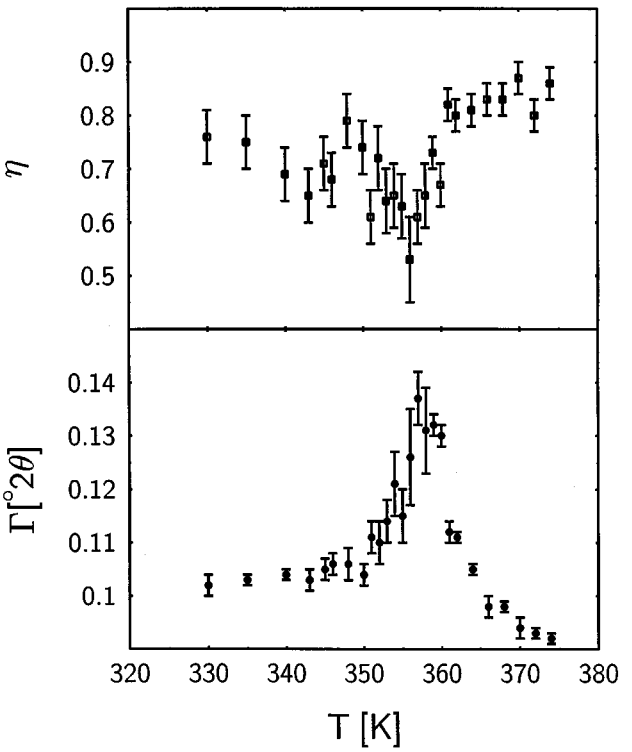

FIG. 6. Change of the full width a half maximum and the pseudoVoigt parameter η for the (004) reflection at the cubic/tetragonal phase transition in D3C-THF.

Applying the volume strain ε_v given by (16) for the symmetrically very similar case of leucite,

$$\varepsilon_0 = \sqrt{3}\,\frac{a_0 - a_0^{\mathrm{id}}}{a_0^{\mathrm{id}}}, \qquad [4]$$

the pure ferroelastic strain $\varepsilon_f = \varepsilon - \varepsilon_v$ can be determined. The values of the strain components are given in Fig. 5.

The total spontaneous strain is small (6×10^{-3} at 330 K). The ferroelastic strain amounts to nearly twice the volume strain. The total and the pure ferroelastic strain change discontinuously to zero at the transition temperature T_c. In contrast, the volume strain seems to decrease almost continuously (*cf.*, inset Fig. 4), at least within the accuracy of the experiment.

The temperature evolution of the peak shape parameters, namely the full width at half maximum (FWHM) and the pseudoVoigt parameter η of the pseudocubic 004 reflection, show an anomaly around T_c (Fig. 6). The FWHM is larger in the tetragonal room-temperature phase than in the cubic high-temperature phase. The FWHM increases from both sides of the transition and shows a discontinuity at T_c.

Symmetry Reduction and Twin Domains

The symmetry reduction at the cubic/tetragonal phase transition in D3C-THF can be expressed by a group/subgroup diagram in steps of maximal subgroups (17), as given in Fig. 7. The tetragonal space groups $I4_1/amd$ and $I4_1/a$ have the same primitive cell as the face-centered cubic cell of the high-temperature phase. Therefore they are termed *translationengleich*. The index 6 of the group/subgroup relation follows from Fig. 7 and corresponds to the number of differently oriented twin domains which may be obtained through the transition (18).

The change of the crystal family comes with a loss of symmetry elements in the high-temperature 'para'-phase. These symmetry elements appear as the twin elements in the low-temperature 'ferro'-phase. According to the index 3 at the $Fd\bar{3}m$–$I4_1/amd$ transition, corresponding to the change of the point groups $m\bar{3}m$–$4/mmm$, three ferroelastic twin domains can be expected at room temperature with the threefold axes of the point group $m\bar{3}m$ as twin elements.

Further symmetry reduction from $4/mmm$ to $4/m$ causes the loss of either the $\{100\}$ or the $\{110\}$ mirror planes of point group $4/mmm$. These planes are part of the holohedry, *i.e.*, the Laue class of highest symmetry for a given crystal family. The resulting twins are called merohedral, and the total number of domains at room temperature is thus six.

Based on the existence of these domains we have to classify the transition according to Aizu's notation (19) as partially ferroelastic. At present, we have no experimental evidence for the existence of an intermediate phase with

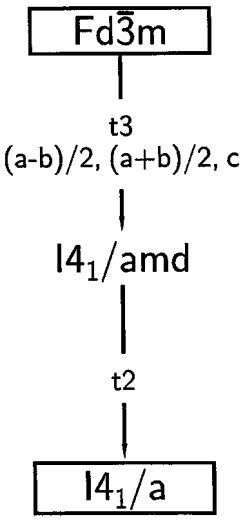

FIG. 7. Group/subgroup diagram for the cubic/tetragonal transition in D3C-THF.

symmetry $I4_1/amd$ in D3C-THF. Therefore, we restrict the following discussion to a direct transition from $m\bar{3}m$ to $4/m$.

Order Parameter Symmetry

Landau theory, as discussed for instance by Janovec and coauthors (20), requires the introduction of a quantity called order parameter (Q). This quantity transforms according to an irreducible representation of the high-symmetry space group. If a suitable macroscopic physical property (spontaneous strain, polarization) transforms accordingly, the phase transition may be considered to be driven by the corresponding tensorial property.

Following (20), the transition $m\bar{3}m$–$4/m$ is characterized by an order parameter Q, which transforms according to the three-dimensional T_{1g} irreducible representation of $m\bar{3}m$. The basis functions for the e_3 unit vector are $\bar{z}$ and $(x^2 - y^2)[xy]$. This method also yields 3 as the total number of crystallographic equivalent low-symmetry groups; the total number of domains is 6. There are no proper components of the spontaneous strain. Improper components of the spontaneous strain are U_1 with $u_{xx} = u_{yy} = -2u_{zz}$, and the symmetry-allowed volume distortion δU_c with $\delta u_{xx} = \delta u_{yy} = \delta u_{zz}$. U_1 corresponds to our experimentally determined ferroelastic strain ε_f, and δU_c to the volume strain ε_v. The transition is classified as improper ferroelastic and thus not driven by the spontaneous strain, which is, however, a secondary order parameter. The primary order parameter for this type of transition has been given by Tolédano and Tolédano (21) and is represented by a fourth rank tensor. The phase transition is driven by an instability of the elastic constants c_{16}–c_{26}. The faintness index of the $Fd\bar{3}m$ to $I4_1/a$ transition is 2 (21).

The thermodynamic potential L of the transition results from the common form of the Landau potential for the three-dimensional order parameter $Q(Q_1, Q_2, Q_3)$ with T_{1g} symmetry (15) and $Q_1 = Q_2 = 0$:

$$L = \tfrac{1}{2}A(T - T_c)Q^2 + \tfrac{1}{4}bQ^4 + \tfrac{1}{6}cQ^6. \qquad [5]$$

In lowest order, the ferroelastic spontaneous strain couples linear-quadratically to the order parameter, $Q^2 \propto \varepsilon_f$. According to Salje (15), for the excess volume strain ε_v all coupling terms $\varepsilon^m Q^n$ with $m = 1$ and n the exponents in Eq. [5] are symmetry-allowed.

Spontaneous strain and optical birefringence are related to each other by the elasto-optic effect. This proportion has been worked out in detail for the case of leucite (22). While $\varepsilon \propto Q^2$, the relation for the optical birefringence is $n \propto (Q^2)^2$. This can be seen easily from the plot of the squared spontaneous strain vs the optical birefringence, which yields an almost linear relationship (Fig. 8). Thus, an exponent $\beta \approx 0.11$ follows from the proportions given above and Eq. [1]. Accordingly, the transition has to be classified as a first order transition. However, first order phase transitions are characterized by a region of coexistence between high-temperature 'para'-phase and low-temperature 'ferro'-phase. Thus, no exact transition temperature or critical exponents can be given at all. Nonetheless, the application of $2\beta = 0.22$ in Eq. [1] yields the curve in Fig. 5 for the total strain, which is in overall good agreement with our experimental data. For a more thorough discussion of the temperature evolution of the strain components, the quality of the data does not suffice.

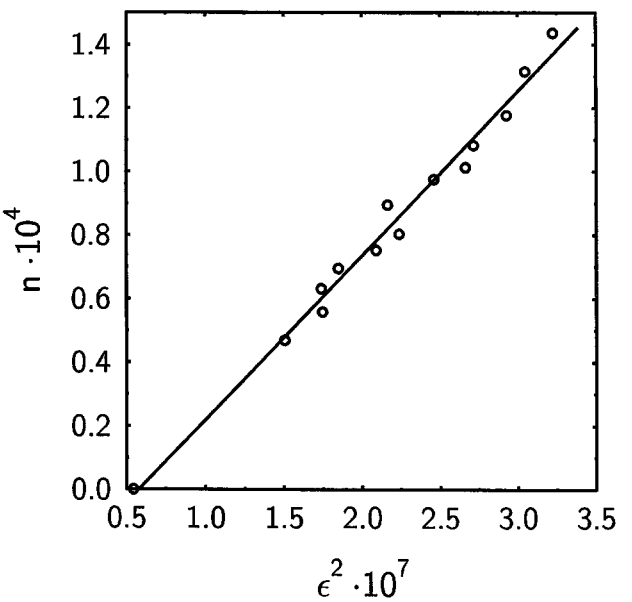

FIG. 8. Plot of the birefringence n vs squared total strain ε^2 for the cubic/tetragonal transition in D3C-THF.

The change of the peak shape parameters as a function of temperature (*cf.*, Fig. 6) might be related to crystal imperfections, mainly the occurrence of domain boundaries. A comprehensive discussion of the origins of line-profile shapes and breadths in powder diffraction is given by Delhez *et al.* (23). As they point out, mainly crystallite size and strain broadening can be distinguished. These properties are usually determined from the Gaussian integral width β_G and from the width of the Lorentzian part β_C of a Voigt peak-shape function, respectively. As described in the experimental section, the use of a split-type pseudoVoigt function was necessary for an appropriate description of the peak shape in our case. The transformation of the full width at half maximum and the η parameter of the pseudoVoigt function into the integral widths of the Gaussian and Lorentzian part of a corresponding Voigt function was given by de Keijser *et al.* (24). The resulting temperature dependence for the integral width of the pseudoVoigt function β^{PV} is given in Fig. 9, together with the evolution of the integral widths for the Lorentzian β_C and Gaussian β_G contribution to the corresponding Voigt function. While strain-broadening is proportional to β_G, size-broadening scales with β_C^{-1} (24).

From β_C in Fig. 9, it follows that coherently scattering regions are of equal size in the 'para'- and 'ferro'-phase, while at around 359 K an increase of the integral width corresponding to a decrease of the crystallite size can be observed. Strain-broadening at the transition follows from the slope of the β_G curve at around 359 K. The difference in the integral width β^{PV} between 'ferro'- and 'para'-phase can be found for the Gaussian part β_G as well, and is interpreted as residual stress in the low-temperature 'ferro'-phase.

Finally, the above-described symmetry changes at the cubic/tetragonal phase transition in D3C-THF find their correspondence in the structural changes through the transition (9). The action of a one-dimensional local tilt system violates the symmetry of the 'para'-phase. The axes of the tilt system run through the centers of only the Si(5) tetrahedra and coincide with the $\bar{4}$ inversion axes of the space group $I4_1/a$. A counter-clockwise rotation of these Si(5) tetrahedra is cooperative only with respect to the next neighboring tetrahedra. Being one-dimensional, the tilt is not transferred to the framework as a whole, and therefore termed local. The transition, governed by this local tilt system, is connected with the removal of the cubic (..*m*) or tetragonal (.*m*.) mirror planes, respectively. Thus the space group $I4_1/a$ is the highest possible symmetry compatible with that tilt system.

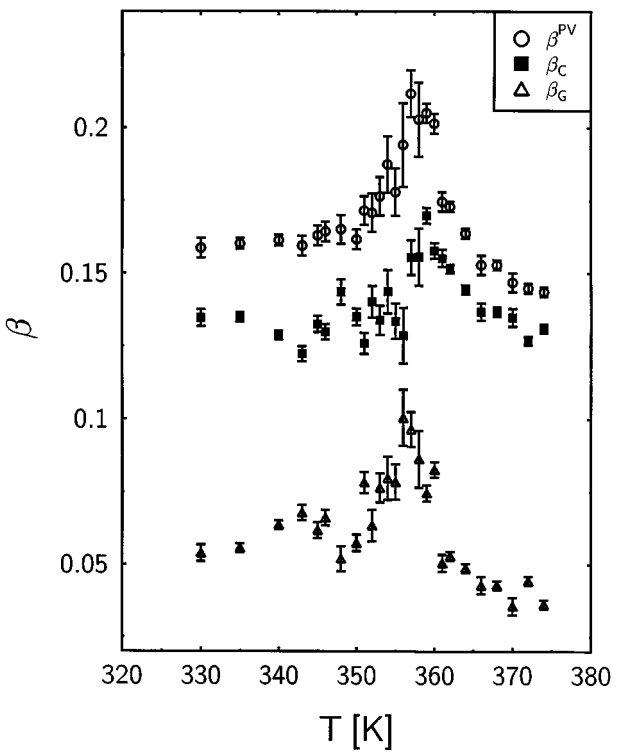

FIG. 9. Temperature dependence of the pseudoVoigt integral breadth β^{PV}, the Cauchy β_C, and the Gaussian β_G contribution of a Voigt function for the (004) reflection of D3C-THF.

ACKNOWLEDGMENTS

The authors would like to thank Prof. H. Gies for supplying the crystals of D3C-THF and Mr. Reuf (TU Berlin) for preparation of the single crystal. Financial support of this work by the Deutsche Forschungsgemeinschaft (Contract DE 412/5–1,2) is gratefully acknowledged.

REFERENCES

1. F. Liebau, "Structural Chemistry of Silicates: Structure, bonding and classification." Springer-Verlag, Berlin, Heidelberg, 1985.
2. H. Gies, F. Liebau, and H. Gerke, *Angew. Chemie* **94,** 214 (1982).
3. J. L. Schlenker, F. G. Dwyer, F. F. Jenkins, W. J. Rohrbaugh, and G. T. Kokotailo, *Acta Crystallogr. Sect. A* **37,** C-377 (1981).
4. H. Gies, *Z. Kristallogr.* **167,** 73 (1984).
5. M. Könnecke, G. Miehe, and F. Fuess, *Z. Kristallogr.* **201,** 147 (1992).
6. H. K. Chae, W. G. Klemperer, D. A. Payne, C. T. A. Suchicital, D. R. Wake, and D. R. Wilson, *in* "New Materials for Nonlinear Optics" (S. R. Marder, J. E. Sohn, and G. D. Stucky, Eds.) ACS Symp. Ser. 455, Am. Chem. Soc., Washington, DC, 1991.
7. M. Könnecke, PhD thesis, Darmstadt, 1991.
8. M. Könnecke and H. Fuess, *Zeolites* **15,** 264 (1995).
9. K. Knorr and W. Depmeier, *Acta Crystallogr. Sect. B* **53,** 18 (1997).
10. J. A. Ripmeester, M. Desando, Y. P. Handa, and J. S. Tse, *J. Chem. Soc., Chem. Commun.* **608** (1988).
11. J. S. Tse, M. Desando, J. A. Ripmeester, and Y. P. Handa, *J. Am. Chem. Soc.* **115,** 281 (1993).
12. L. Cemić, St. Grammenopoulou-Bilal, and K. Langer, *Ber. Bunsen-Ges. Phys. Chem.* **90,** 654 (1986).
13. X. Hu, PhD thesis, Berlin, 1993.
14. H. Toraya, PRO-FIT, Ceramic Engineering Research Laboratory, Nagoya Institute of Technology, 1990.
15. E. K. H. Salje, *in* "Phase Transitions in Ferroelastic and Co-elastic Crystals," Cambridge Topics in Mineral Physics and Chemistry 1, (A. Putnis and R. C. Liebermann, Eds.), Cambridge University Press, Cambridge, 1990.

16. D. C. Palmer, E. K. H. Salje, and W. Schmahl, *Phys. Chem. Miner.* **16,** 714 (1989).
17. H. Bärnighausen, *Commun. Math. Chem.* **9,** 139 (1980).
18. H. Wondratschek and W. Jeitschko, *Acta Crystallogr. Sect. A* **32,** 664 (1976).
19. K. Aizu, *Phys. Rev. B* **2,** 754 (1970).
20. V. Janovec, V. Dvorak, and L. Petzelt, *Czech. J. Phys.* **25,** 1362 (1975).
21. J. C. Tolédano and P. Tolédano, *Phys. Rev. B* **21,** 1139 (1980).
22. D. C. Palmer, U. Bismayer, and E. K. H. Salje, *Phys. Chem. Miner.* **17,** 259 (1990).
23. R. Delhez, T. H. de Keijser, J. I. Langford, D. Louër, E. J. Mittemeijer, and E. J. Sonneveld, "Crystal imperfection broadening and peak shape in the Rietveld method," *in* "The Rietveld method," (R. A. Young, ed.), Oxford University Press, New York, 1996.
24. T. H. de Keijser, E. J. Mittemeijer, and H. C. F. Rozendaal, *J. Appl. Crystallogr.* **16,** 309 (1983).